Monthly Notices of the ROYAL ASTRONOMICAL SOCIETY

Mon. Not. R. Astron. Soc. **427,** 2392–2400 (2012) doi:10.1111/j.1365-2966.2012.22071.x

A study of the orbits of the logarithmic potential for galaxies

S. R. Valluri,[1,2,3★] P. A. Wiegert,[1] J. Drozd[4] and M. Da Silva[1]

[1]*Department of Physics and Astronomy, Western University, London, Ontario N6A 3K7, Canada*
[2]*Department of Applied Mathematics, Western University, London, Ontario N6A 5B7, Canada*
[3]*King's University College, London, Ontario N6A 2M3, Canada*
[4]*Robarts Research Institute, London, Ontario N6A 5K8, Canada*

Accepted 2012 September 5. Received 2012 August 3; in original form 2011 October 27

ABSTRACT

The logarithmic potential is of great interest and relevance in the study of the dynamics of galaxies. Some small corrections to the work of Contopoulos & Seimenis who used the method of Prendergast to find periodic orbits and bifurcations within such a potential are presented. The solution of the orbital radial equation for the purely radial logarithmic potential is then considered using the precessing ellipse (p-ellipse) method pioneered by Struck. This differential orbital equation is a special case of the generalized Burgers equation. The apsidal angle is also determined, both numerically and analytically by means of the Lambert *W* and the polylogarithmic functions. The use of these functions in computing the gravitational lensing produced by logarithmic potentials is discussed.

Key words: celestial mechanics – galaxies: kinematics and dynamics.

1 INTRODUCTION

The logarithmic potential is of great interest in connection with the study of the dynamics of elliptical galaxies and galactic haloes. Introduced by Richstone (1980) to model stellar systems with concentric axisymmetric oblate spheroidal potential surfaces, it is one of the few axisymmetric galactic potentials with an equally simple mass distribution function. As a result, it has been studied extensively (e.g. Binney & Spergel 1982; Binney & Tremaine 1987).

Richstone (1982) did an extensive survey of orbits within scale-free logarithmic potentials (i.e. with zero core radii). The effect of the core radius and the presence or absence of a central mass has been examined by Gerhard & Binney (1985), Pfenniger & de Zeeuw (1989) and Miralda-Escude & Schwarzschild (1989). Evans (1993) examined the axisymmetric case of galaxies embedded in extended dark matter haloes. Lees & Schwarzschild (1992) examined triaxial halo models. Karanis & Caranicolas (2001) examined how the core radius and the angular momentum are related to transitions from regular motion to chaos in logarithmic potentials. Touma & Tremaine (1997) developed a symplectic map to study the dynamics of orbits in non-spherical potentials, with particular emphasis on the logarithmic potential. Periodic orbits in triaxial logarithmic potentials have been examined analytically (Belmonte, Boccaletti & Pucacco 2007; Pucacco, Boccaletti & Belmonte 2008) and numerically (Magnenat 1982).

Beyond galactic dynamics, the potential also has applications to the problem of gravitational lensing. Beyond astrophysics, applications of the logarithmic potential occur in the solution of planar boundary value problems in potential theory (Evans 1927) and boundary value problems in analytic function theory. In elementary particle physics, Quigg & Rosner (1977) use the logarithmic potential to show that the quarkonium level spacings are independent of quark mass, in the non-relativistic limit. In this paper, the analysis of (Contopoulos & Seimenis 1990, hereafter CS) is re-examined. CS applied the analytical techniques of Prendergast (1982) to find approximate solutions to the equations of motion for particles moving within a logarithmic potential. The Prendergast method was introduced to approximate some complex differential equations, such as the Duffing equation, and new applications for this method are still being found today. We then elaborate on the work of CS, turning our attention to the radial orbital equation, using the non-linear Burgers equation to determine an approximate analytic solution from which the apsidal angle is determined. It is also determined by finding the roots of the Lambert *W* and the polylogarithmic functions.

In Sections 2 and 3, the Prendergast method is revisited. We performed a thorough study of the pioneering work of CS and present a slight elaboration as well as a few minor corrections to their equations. In Section 4, we briefly study Struck's (2006) precessing ellipse (p-ellipse), introduced in his fine work on precessing orbits in a variety of power-law potentials, some shallower than the $1/r$ Keplerian one. These potentials include the logarithmic potential of zero as well as non-zero core softening length. We present an integrable equation that provides us with values for the apsidal angles of the orbits considered. In Section 5, we discuss the deflection of light in a logarithmic potential and gravitational lensing. Finally, Section 6 summarizes our conclusions and any further work to be considered.

★E-mail: valluri@uwo.ca

2 UNPERTURBED SOLUTIONS

Here we begin by re-establishing the results of CS with some minor corrections, before going on to use these solutions in subsequent sections. Where alterations to their values are given, they are indicated by asterisks.

Following the notation of CS, our expression for the logarithmic potential is

$$V(x, y) = \ln\left(x^2 + \frac{y^2}{U^2} + C^2\right), \tag{1}$$

where C is the core radius and U describes the ellipticity of the potential. Though of mathematical interest over a wider range of parameters, models with $U > 1.08$ or $U < 1/\sqrt{2} = 0.707$ are unphysical in that they require negative mass densities (Evans 1993). As a result, only values of $0.707 < U < 1.08$ are of interest to galactic dynamics. The CS method begins by finding a solution for arbitrary values of U in the one-dimensional case ($y \equiv \dot{y} \equiv 0$), and adding the motion in the second dimension as a perturbation.

By finding the derivative of equation (1) and introducing it in the relevant second-order orbital differential equation, it is possible to develop two equations of motion – one for the x component and the other for the y component:

$$x'' + \frac{2U^2x}{U^2x^2 + y^2 + C^2U^2} = 0, \tag{2}$$

$$y'' + \frac{2y}{U^2x^2 + y^2 + C^2U^2} = 0 \quad (*), \tag{3}$$

where the $(*)$ indicates the equation contains a correction to a typo in CS's original.

The subsequent solution is developed using the method of Prendergast (1982). Developed for second-order non-linear ordinary differential equations, Prendergast applied the technique to the van der Pol oscillator and Duffing's equation. CS applied it to the orbital equation in the logarithmic potential.

The method begins by assuming a solution for x and y of the following form:

$$x = \frac{N}{D}, \qquad y = \frac{M}{D}, \tag{4}$$

where N, M and D are Fourier series of the form

$$\begin{aligned} N &= \sum_{k=\text{odd}} N_k \cos(k\omega t), \\ D &= 1 + \sum_{l=\text{even}} D_l \cos(l\omega t), \end{aligned} \tag{5}$$

and which are truncated at an appropriate order. In the unperturbed one-dimensional case, $y = \dot{y} = 0$ and $M = 0$.

In determining the solution for x, we substitute equations (4) into equation (2), and solve for a new equation of motion,

$$\begin{aligned} &\left(N''D^2 - 2N'D'D - ND''D + 2ND'^2\right) \\ &\quad \times \left(U^2N^2 + M^2 + C^2U^2D^2\right) + 2U^2ND^4 = 0. \end{aligned} \tag{6}$$

A solution is essayed of the form

$$N = A\cos(\omega t), \quad D = 1 + B\cos(2\omega t), \tag{7}$$

with the constants A, B and ω to be determined, though we require $B \neq 0$ for a non-trivial rational approximation.

Finally, we substitute the proposed solutions (7) into equation (6) and set equal to zero the coefficients of $\cos(\omega t)$ and $\cos(3\omega t)$. This gives us two equations:

$$\begin{aligned} \omega^2k_1 + 0.75B^4 + 3B^3 + 6B^2 + 4B + 2 = 0, \\ \omega^2k_2 + 0.5B^4 + 3B^3 + 3B^2 + 4B = 0, \quad (*) \end{aligned} \tag{8}$$

where k_1 and k_2 are as given below:

$$\begin{aligned} k_1 = {} & 3.5625A^2B^2 + 7B^2C^2 + 2.125C^2B^4 \\ & - 2BC^2 + 3.5C^2B^3 - 0.75A^2 - C^2, \end{aligned} \tag{9}$$

$$\begin{aligned} k_2 = {} & 0.1875A^2B^2 + 1.25A^2B - 0.25A^2 \\ & + 6.5C^2B^3 - 3.5B^2C^2 + 2BC^2 + 0.25C^2B^4. \quad (*) \end{aligned} \tag{10}$$

The third equation needed to determine A, B and ω is given by the initial condition

$$(1 + B)x_0 - A = 0, \tag{11}$$

where $x_0 \equiv x(t = 0)$.

We now solve these equations for A, B and ω with the given values of x_0. The solutions, as well as all mathematical manipulations presented in this paper, unless otherwise mentioned, were determined using the software package MAPLE 15. The solutions have $\omega^2 > 0$ and are presented in Table 1.

We note that for motion solely in the x-direction the value of U is irrelevant, and it appears neither in equation (8) nor in the initial conditions.

An example of an unperturbed solution is shown in Fig. 1 with values corresponding to line 17 in Table 1.

Table 1. A comparison of our results with those of Contopoulos & Seimenis (1990). Where a corrected value appears, the original value appears in brackets below it.

	x_0	A	B	ω
1	0.001	0.001 000 006	6.2497E−6	14.142
2	0.01	0.010 006 216 94	0.000 621 693 5078	14.089
3	0.02	0.020 048 955 06	0.002 447 752 803	13.935
4	0.03	0.030 160 977 74	0.005 365 924 678	13.689
5	0.04	0.040 368 177 27	0.009 204 431 71	13.368
6	0.05	0.05068761968	0.01375239358	12.989
7	0.06	0.061 127 008 08	0.018 783 468 08	12.569
8	0.07	0.071 685 497 91 (0.024 074)	0.024 078 541 58*	12.125
9	0.08	0.082 355 498 42 (0.029 436)	0.029 443 73*	11.668
10	0.09	0.093 124 932 32* (0.093 124)	0.034 721 47* (0.034 708)	11.211
11	0.1	0.103 979 4453* (0.103 977)	0.039 794 453* (0.039 775)	10.761
12	0.125	0.131 392 83* (0.131 388)	0.051 142 64* (0.051 102)	9.696
13	0.15	0.159 049 8684* (0.159 040)	0.060 332 456* (0.060 266)	8.747
14	0.175	0.186 818 5967* (0.186 803)	0.067 534 838* (0.067 443)	7.921
15	0.2	0.214 624 6114* (0.214 602)	0.073 123 057* (0.073 008)	7.210* (7.209)
16	0.225	0.242 430 1778* (0.242 400)	0.077 467 457* (0.077 332)	6.597
17	0.25	0.270 217 96* (0.270 180)	0.080 871 84* (0.080 719)	6.068

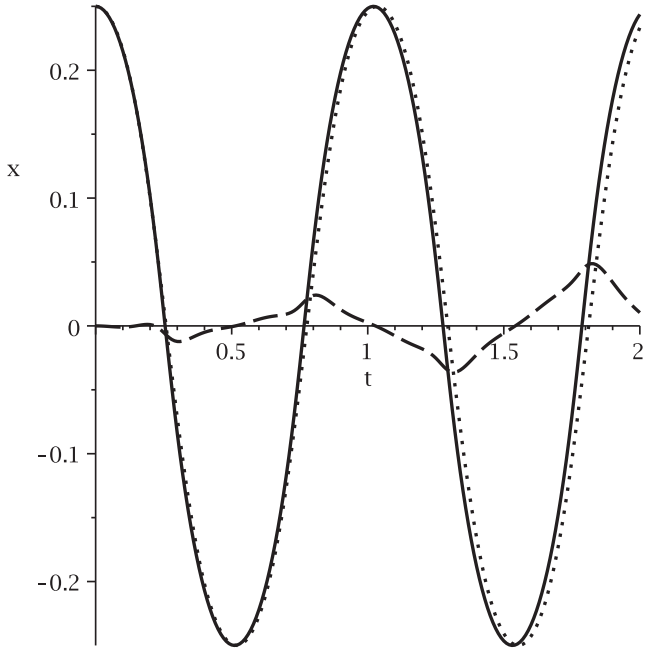

Figure 1. A typical solution showing x versus time for the unperturbed solution based on the values of line 17 in Table 1. The solid line is the numerical solution from MAPLE 15, the dotted line is our approximation and the dashed line is the difference between the two.

3 PERTURBED SOLUTIONS

Purely radial orbits such as those of Section 2 are unlikely in practice. Here the search is for solutions to the motion where the y component of the motion is close to the unperturbed motion discussed previously. In this case, M is no longer identically zero and we look for solutions of the form

$$M = M_0 + \delta M, \quad D = D_0 + \delta D, \quad N = N_0 + \delta N, \tag{12}$$

where the subscript 0 indicates the unperturbed solution. The next step is to solve the differential equation, introduced as equation (8) in CS,

$$\begin{aligned} &\left(U^2N^2D^2 + C^2U^2D^4\right)\delta M'' \\ &- \left(2U^2N^2DD' + 2C^2U^2D^3D'\right)\delta M' \\ &+ \left(2U^2N^2D'^2 - U^2N^2DD'' - C^2U^2D^3D'' \right. \\ &\left. + 2C^2U^2D^2D'^2 + 2D^4\right)\delta M = 0. \end{aligned} \tag{13}$$

The proposed solutions from equation (5) are substituted into equation (13) and solutions of the form

$$\delta M = \sum_{k=-\infty}^{\infty} C_k \cos\left((\nu + k)\,\omega t\right) \tag{14}$$

are searched for, where ν is a constant. CS determined from Floquet's (1883) work that values outside the range $0 \leq \nu \leq 1/2$ are unstable, and thus $\nu(x_0) = 0$ and $\nu(x_0) = 1/2$ bracket the stable region. They found no solution in the case of $\nu = 0$, but solutions do exist for the case $\nu = 1/2$, discussed below.

In order to get a finite number of non-trivial solutions, equation (14) must be truncated after a finite number of terms. Following CS we consider

$$\delta M = \sum_{k=-3}^{2} C_k \cos\left(\left(k + \frac{1}{2}\right)\omega t\right), \tag{15}$$

which leaves us with six values of C_k to be determined.

The main goal here is to solve for the six constants C_k. In order to do this, we substitute equation (15) and its derivatives into equation (13), as well as the corresponding substitutions for N and D. From this point onwards, we diverge from the treatment of CS, as here we have used different methods to find this equation's solutions. Here we have used MAPLE 15 and MATHEMATICA 8 as the tools for equation solving.

(1) Using MAPLE's COMBINE function, equation (13) was solved for one value of C_k. The solution revealed many cosine terms with different frequencies, and some terms that were totally independent of the cosine.

(2) The three lowest frequencies of cosine (including the independent terms when present) were factored out of each individual C_k term. The terms relating to a single frequency were collected, yielding three separate equations. The cosine was then factored out, and the remainder of the equations set equal to zero.

(3) Steps (1) and (2) were repeated for each individual term of C_k. The result was 18 equations where there were three equations for each C_k (each of the three equations representing a different frequency of cosine). Using these equations, a 6×6 matrix results, where rows 1, 3 and 5 represent equations with k values of -3, -1, 1 and rows 2, 4 and 6 represent equations with k values of -2, 0, 2, respectively:

$$\begin{bmatrix} S_{11} & 0 & S_{13} & 0 & S_{15} & 0 \\ 0 & S_{22} & 0 & S_{24} & 0 & S_{26} \\ S_{31} & 0 & S_{33} & 0 & S_{35} & 0 \\ 0 & S_{42} & 0 & S_{44} & 0 & S_{46} \\ S_{51} & 0 & S_{53} & 0 & S_{55} & 0 \\ 0 & S_{62} & 0 & S_{64} & 0 & S_{66} \end{bmatrix} \tag{16}$$

In other words, the columns are in increasing order from -3 to 2, which demonstrates which equations contain which k values.

We now solved the equations in sets of three for the values of C_k. In essence, we constructed equations from the matrix (e.g. $S_{11} + S_{13} + S_{15} = 0$ and so forth down the rows). Rows 1, 3 and 5 were used to solve for C_{-3}, C_{-1} and C_1. Similarly, rows 2, 4 and 6 were used to solve for C_{-2}, C_0 and C_2. The two homogeneous sets of three equations were transformed to two non-homogeneous systems of order 2 with C_{-1} and C_0 set equal to unity for mathematical convenience.

Once all six coefficients were determined, the values for $x(t)$ and $y(t)$ could be determined for specific sets of values of A, B and ω from Table 1. We then use the relations $u = \frac{1}{r}$ and $r = \sqrt{x^2 + y^2}$ to solve for u.

Fig. 2 shows two examples of a perturbed solution. In the left-hand panel, a parametric plot in t of x versus y for parameters $U = 2/3$, $C = 0.1$, and other values corresponding to line 1 in Table 1 are shown. Here the initial value of y is taken to be 10^{-4} to justify our assumption that it is small. The two solutions are so similar that the graphs overplot each other and cannot be distinguished. The right-hand panel shows a much larger orbit based on the parameters in line 17 of Table 1. Here the Prendergast solution does not contain enough frequency information to completely reproduce the box orbit but captures some of the character of the true solution, such as the x and y amplitudes and period.

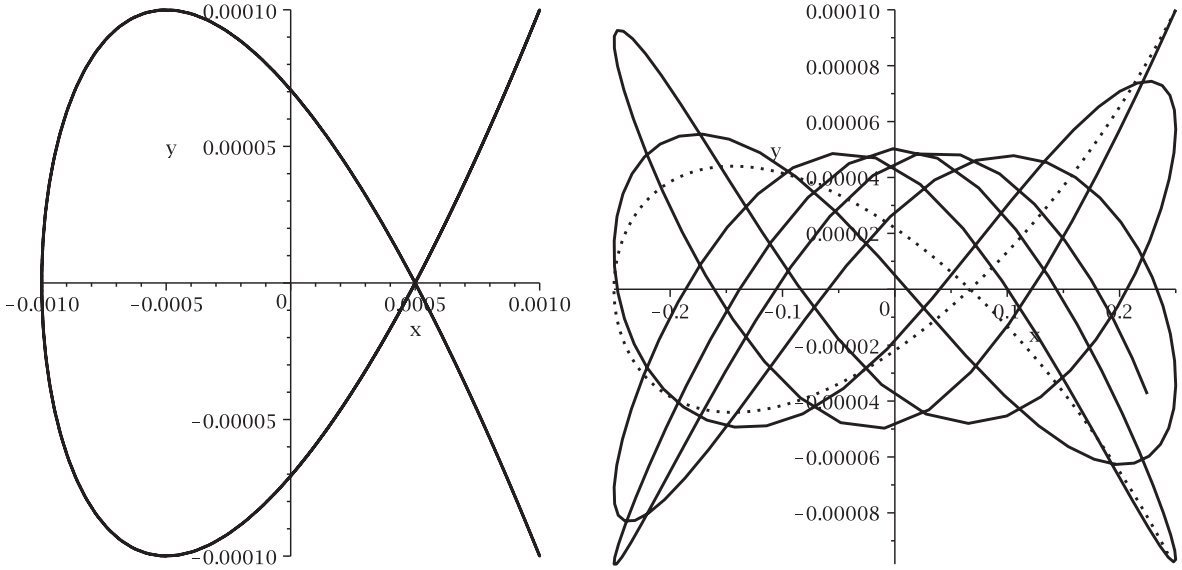

Figure 2. Two solutions showing x and y as a parametric curve in t. The left-hand panel shows the Prendergast and real solutions based on the values of line 1 in Table 1. The two solutions are plotted on top of each other at this resolution and cannot be distinguished. The right-hand panel shows a larger orbit, corresponding to the values of line 17 in Table 1. The solid curve is the numerical solution from MAPLE 15 over four cycles and the dotted line is the Prendergast approximation.

4 THE APSIDAL ANGLE AND P-ELLIPSE ORBITS

In this section, we turn our interest to the approximate solution of the radial orbital differential equation. We are primarily interested in the precession of the apsidal angle, and so we will consider the problem now in terms of the anomaly θ rather than the time t. If one wishes to determine the relationship between these two variables, a Kepler-like equation would need to be solved.

CS considered the x and y equations of motion, but here we consider $u = 1/\sqrt{x^2 + y^2} = 1/r$ with an eye to later using this result to determine the apsidal angle for the purely radial logarithmic potential. In this case, we examine the case where $U \approx 1$ and $C \ll 1$. We start with the radial orbital differential equation, which is of the form

$$\frac{\mathrm{d}^2u}{\mathrm{d}\theta^2} + u = -\frac{1}{h^2u^2} f\left(\frac{1}{u}\right), \tag{17}$$

where h is the angular momentum. We note that the force function $f(\frac{1}{u})$ is equal to $-\mathrm{d}V/\mathrm{d}r$, which can be obtained by differentiating equation (1).

The Prendergast method works very well for the solutions of the logarithmic potentials from equation (1) indicated in Section 2 for the x and y equations of motion and further elaborated in Section 3. However, the method does not seem to be well suited for purely radial logarithmic potentials with different initial conditions, and the solution does not agree with that obtained by pure numerical integration of the orbital differential equation. The p-ellipse approximate solutions of the orbital equation, pioneered by Struck (2006), are a much better way of not only deriving an accurate approximate solution of order e^2 (where e is the orbital eccentricity), but also obtaining the values for the apsidal precession to a high accuracy. We present a detailed analysis of the orbital equation for the radial logarithmic potential with or without the inclusion of the core scalelength. In our analysis, the factor $0 \leq C \leq 1$ gives a measure of the core scalelength (Struck 2006).

For the case of large orbits, or negligible core size softening length, the equation of motion is given by

$$uu'' + u^2 = c\,, \tag{18}$$

where the parameter c, in the notation of Struck, depends both on the constant scale mass M^* and on the core scalelength ε of the potential, the gravitational constant G and the angular momentum h. The above equation is similar to equation (17), and of the form

$$u'' + u = \frac{c}{u}. \tag{19}$$

Struck suggested an approximate solution of equation (19):

$$u = \frac{1}{p}\left\{1 + e\cos\left[(1-b)\,\phi\right]\right\}^{1/2}, \tag{20}$$

where $p = a(1 - e^2)$ is the semilatus rectum (a being the semi-major axis) (e.g. Murray & Dermott 1999; Valluri et al. 2005), e is the orbital eccentricity and $(1 - b)$ is the factor associated with the precession rate. Henceforth, for convenience, we set $k = 1 - b$ in our analysis, and we will use θ instead of ϕ as was used by Struck.

Struck finds that orbits obtained from a numerical integration of the above differential equation look like p-ellipses and considers the approximate solution given in equation (20).

Substituting the solution of equation (20) into the differential equation, we find

$$-\frac{k^2}{2p^2}\left[-\frac{e^2-1}{2\,(1+e\cos k\theta)} + \frac{1+e\cos k\theta}{2}\right] + \frac{1+e\cos k\theta}{2p^2} = c, \tag{21}$$

$$\therefore uu'' + u^2 = \frac{k^2}{2p^2}\,\frac{1 - e^2 + \frac{1}{p^2}\left(1 - \frac{k^2}{4}\right)(1 + e\cos k\theta)}{2(1 + e\cos k\theta)} = c\,. \tag{22}$$

The left-hand side of equation (22) simplifies to

$$uu'' + u^2 = -\frac{1}{2p^2}(1 + e\cos k\theta) + \frac{1}{p^2}(1 + e\cos k\theta) + \frac{1}{2p^2}\left(1 - e^2\right)\frac{1}{1 + e\cos k\theta} = c\,, \tag{23}$$

where $c_1 = \frac{1}{2p^2} + \frac{1}{2p^2} = \frac{1}{p^2}$ and $k^2 = (1 - b_1)^2 = 2$ are the first approximations to c and k, respectively (Struck 2006). In a more accurate approximation of order e^2, we find that the constant terms reduce to

$$\frac{k^2}{4p^2}\left(1 - e^2\right) - \frac{k^2}{4p^2} + \frac{1}{p^2} = c\,. \tag{24}$$

Next, comparing the terms involving $\cos k\theta$, we find that the coefficient of $\cos k\theta$ is given by

$$-\frac{k^2}{4p^2}e\left(1 - e^2\right) - \frac{k^2 e}{4p^2} + \frac{e}{p^2} = 0\,. \tag{25}$$

On simplification, one obtains

$$k^2 = \frac{2}{1 - \frac{1}{2}e} = 2\left(1 + \frac{e}{2} + \frac{e^2}{4}\right)\,. \tag{26}$$

For $e = 0$, $k^2 = 2$ in accordance with Struck (2006).

In the case of non-negligible core size, one has a similar though modified differential equation of the form

$$\left(uu'' + u^2\right)\left(1 + u^2\right) = c\,. \tag{27}$$

The solution given in equation (20) upon substitution into the above differential equation leads to the expression

$$\left[-\frac{k^2}{4p^2}(1 + e\cos k\theta) + 1 + \frac{e\cos k\theta}{p^2} + \frac{k^2}{4p^2}\frac{\left(1 - e^2\right)}{1 + e\cos k\theta}\right] \times \left(1 + \frac{1 + e\cos k\theta}{p^2}\right) = c \tag{28}$$

which, upon comparison of terms independent of $\cos k\theta$, simplifies to

$$\frac{1}{p^2}\left(1 - \frac{k^2e^2}{4}\right)\left(1 + \frac{1}{p^2}\right) + \frac{k^2}{4p^2}\left(1 - e^2\right)\left(1 + \frac{1}{p^2}\right)\left(-\frac{e^2}{2}\right) + \frac{k^2}{4p^2}\left(1 - e^2\right)\left(-\frac{e^2}{2p^2}\right) = c\,. \tag{29}$$

Comparing the coefficients of $\cos k\theta$, we get the more general dependence of k^2:

$$k^2 = 2\left(1 + \frac{\frac{e^2}{2} + \frac{1}{p^2}}{1 + \frac{1}{p^2} - \frac{e^2}{2}}\right)\,. \tag{30}$$

If the terms of order e^2 are ignored,

$$k^2 = 1 - b_1 = 2\left(\frac{1 + \frac{2}{p^2}}{1 + \frac{1}{p^2}}\right)\,, \tag{31}$$

where b_1 is the first approximation of the precession factor.

Furthermore, of order e^4

$$c = \frac{1}{p^2}\left(1 + \frac{1}{p^2}\right) - \frac{k^2e^2}{4p^2}\left(\frac{3}{2} + \frac{1}{p^2} + \frac{2}{p^2}\right) + \frac{k^2e^4}{8p^2}\left(1 + \frac{2}{p^2}\right) \tag{32}$$

in agreement with Struck.

It is interesting to note that the orbital differential equation associated with apsidal precession is a special case of the generalized Burgers partial differential equations (GBEs) and seems to characterize these equations similar to the way Painleve equations represent the Korteweg–de Vries type of equations (Sachdev 1991). This variety of equations can be expressed as equations (33) and (34), where $f(x)$ and $g(x)$ are sufficiently smooth arbitrary functions, a, e and c are real constants, and the solutions of y are Euler–Painleve transcendents (Kamke 1943):

$$yy'' + ay'^2 + f(x)yy' + g(x)y^2 + ey' + c = 0\,. \tag{33}$$

In the case where $f(x)$ and $g(x)$ are constants, we have the Euler–Painleve equation

$$yy'' + ay'^2 + byy' + cy^2 + dy^{1-\alpha} = 0\,. \tag{34}$$

For $\alpha = 1, b = 0$, the substitution $y = u^{1/2}$ leads to the differential equation

$$-\frac{1}{4}\frac{u'^2}{u} + \frac{1}{2}u'' + cu + d + \frac{a}{4}\frac{u'^2}{u} = 0\,. \tag{35}$$

For $a = 1$ the $\frac{u'^2}{4u}$ terms cancel, and the following equation results:

$$\frac{1}{2}u'' + cu + d = 0\,. \tag{36}$$

It is important to observe that the orbital differential equation does not have the ay'^2 term in contrast to the GBEs. This term contains terms of order e^2 and the correction does not turn out to be significant. Hence, the p-ellipse is a natural approximate solution of the GBEs and is an Euler–Painleve transcendant (Kamke 1943).

As a rough estimate of the mean error in neglecting the $\frac{u'^2}{4u}$ term, we evaluate the following integrals that occur in the evaluation of this term:

$$-\frac{2k^2e^2}{16p}\frac{1}{e^2}\left[\int_0^{\pi}(1 + e\cos k\theta)^{\frac{1}{2}}\mathrm{d}\theta - \int_0^{\pi}(1 + e\cos k\theta)^{-\frac{1}{2}}\mathrm{d}\theta\right]\,. \tag{37}$$

Substituting $k\theta = x$ we have

$$I_1 = \left[\frac{1}{\pi}\frac{1}{k}\int_0^{k\pi}(1 + e\cos x)^{\frac{1}{2}}\mathrm{d}x\right] = \left[1 + \frac{1}{2}e\frac{\sin k\pi}{k\pi} - \frac{1}{8k\pi}e^2\left(\frac{k\pi}{2} + \frac{\sin 2k\pi}{4}\right) + \cdots\right] \tag{38}$$

and

$$I_2 = \frac{1}{\pi}\frac{1}{k}\int_0^{k\pi}\frac{\mathrm{d}x}{(1 + e\cos x)^{\frac{1}{2}}} = \left[1 - \frac{1}{2}e\frac{\sin k\pi}{k\pi} + \frac{3}{16}e^2 + \frac{3}{16}e^2\frac{\sin 2k\pi}{2k\pi} + \cdots\right]\,. \tag{39}$$

Hence, we obtain for the difference of the two integrals,

$$I_1 - I_2 \approx \left[e\frac{\sin k\pi}{k\pi} - \frac{e^2}{4} - \frac{2e^2}{16}\frac{\sin 2k\pi}{k\pi} + \cdots\right]\,. \tag{40}$$

An approximate mean error (ME) due to the presence of the term $\frac{u'^2}{4u}$ is

$$\mathrm{ME} = \left|-\frac{2k^2}{16\pi}\frac{1}{p}\left[-\frac{0.9e}{k\pi} - \frac{e^2}{4} + \frac{e^2}{16} + \cdots\right]\right|\,. \tag{41}$$

Recalling $p = a(1 - e^2)$ and taking $k \approx 1.45$ and $e \sim 0.9$, we have

$$\mathrm{ME} = \frac{2.9}{16\pi}\frac{1}{0.19a}\left|-\frac{0.81}{4} - \frac{2.43}{16}\right|\,. \tag{42}$$

We find that ME is $\sim$1 per cent for $a = 1$, $e = 0.3$ ($k = 1.79$); ME increases with higher e and decreases with larger a.

Table 2. Some values of the apsidal angle from the p-ellipse prescription ($C = 0$) with varying eccentricity.

a	e	k	θ (rad)
0.75	0.1	1.813 63	1.732 22
0.75	0.5	1.875 98	1.674 64
0.75	0.9	1.990 02	1.578 67
1	0.1	1.734 95	1.810 77
1	0.5	1.811 08	1.734 65
1	0.9	1.982 50	1.584 66
1.5	0.1	1.623 62	1.934 93
1.5	0.5	1.788 58	1.756 47
1.5	0.9	2.172 05	1.446 37
6	0.1	1.437 15	2.185 99
6	0.5	1.535 20	2.046 37
6	0.9	1.984 41	1.583 14

Interestingly, when $k\theta = \pi$ or $k\theta = 0$,

$$\frac{u'^2}{4u} = 0\,, \tag{43}$$

showing that this correction term does not contribute to these angles, as shown below:

$$\begin{aligned}\frac{-(1-e^2)}{(1-e)\,(1-e)^{\frac{1}{2}}} + \frac{1+e}{(1-e)^{\frac{1}{2}}} &= -(1-e^2) + (1+e^2)\\ &= 0\,.\end{aligned} \tag{44}$$

Next, we calculate the apsidal angle for the orbits in a logarithmic potential. The apsidal angle is the angle at the force centre between the smallest and largest apses, that is, between the pericentre and apocentre. Hence, the behaviour of the logarithmic potential is similar to that of the $n > 2$ power-law potentials. Thus, there will always be a single minimum regardless of the value of the constant c. As c increases, the location of the minimum simply shifts to larger x values.

Only bound orbits are possible for this potential. As $x \to \infty$, $V(x)$ also approaches infinity due to the $\ln(x)$ term, so there is always an inner and an outer turning point no matter how large the total energy of the system is. Stable circular orbits are possible at the minimum of the effective potential.

The approximate p-ellipse orbits are, on first appearance, only good to first order in e. However, Struck, in his thorough analysis, has shown that the orbital fits are excellent over several orbital periods. In fact, the value of $k = 1 - b$ which more accurately depends on e is still fairly close to the more exact value, as partly due to the slow variation of c with e. The apsidal angle has been calculated for various values of e and is shown in Table 2.

We now calculate the apsidal angle by using the Lambert W function, a function that is creating a renaissance in solving many interesting problems involving roots and limits of integration, as well as others.

We begin by defining the energy E of an orbit through the summation of its kinetic and potential energies:

$$E = \frac{1}{2}\left[\left(\frac{\mathrm{d}r}{\mathrm{d}t}\right)^2 + r^2\left(\frac{\mathrm{d}\theta}{\mathrm{d}t}\right)^2\right] + V(r)\,, \tag{45}$$

where $r^2\frac{\mathrm{d}\theta}{\mathrm{d}t} = h$ is the angular momentum, and $\frac{\mathrm{d}r}{\mathrm{d}\theta}$ can be broken into $\frac{\mathrm{d}r}{\mathrm{d}u}\frac{\mathrm{d}u}{\mathrm{d}\theta}$.

Our main goal is to solve for $\frac{\mathrm{d}u}{\mathrm{d}\theta}$ as this will provide us with an integrable function from which we can ultimately obtain a value for θ.

Working in the regime where $C \ll 1$ and $U \approx 1$, $V(r)$ can be simplified further and we obtain the following:

$$\frac{\mathrm{d}\theta}{\mathrm{d}u} = \frac{h}{\sqrt{2E + 2\ln u^2 - u^2 A}}\,, \tag{46}$$

where $A = h^2 + 2C^2$ and $E = 0.5 + \ln r_\mathrm{c}$, where r_c is the radius of the circular orbit. The value of $u_\mathrm{c} = 1/r_\mathrm{c}$ is taken here at values between 1 and 1.8, examining a range around the nominal value ($E \approx 0$, $h = e^{-1/2}$) of $u_\mathrm{c} = e^{1/2} \approx 1.648$.

Where $\mathrm{d}\theta/\mathrm{d}u$ passes from positive to negative reveals the location of the apses; thus, the limits of integration of equation (19) are its corresponding roots. We can solve for these roots by setting the denominator equal to zero, and manipulating it so that it can become solvable using the Lambert W function (Valluri, Jeffrey & Corless 2000). We start by reworking the denominator into the following form:

$$\ln u^2 - \frac{u^2}{2}A = -E\,. \tag{47}$$

The roots are given by the expression

$$u = \sqrt{\frac{-2W_j(-\frac{A}{2}e^{-E})}{A}}\,, \tag{48}$$

where W_j represents the Lambert W function and j represents the chosen branch. We solve for the two roots by using the -1 and the zero branches.

Having the apocentre r_M and pericentre r_m distances in hand allows a determination of the orbit eccentricity through

$$\frac{r_M}{r_m} = \frac{1+e}{1-e}. \tag{49}$$

We note that solutions with imaginary eccentricity, which have two complex solutions that are conjugates of each other, would be manifested by a plunging of the orbit into the force centre (Hagihara 1931; Chandrasekhar 1983).

Integrating equation (46) with the two roots as end-points of the integral yields an answer that represents the apsidal angle for the particular orbit with a specific value of u_c.

Fig. 3 shows the apsidal angle calculated by this method, for different values of C, E and h.

Table 3 shows how values of u_c ranging from 1 to 1.8 yield similar apsidal angles with values near $\frac{2\pi}{3}$. For comparison, Touma & Tremaine (1997) use the epicyclic approximation for near-circular orbits to determine that their $g(\alpha, y)$ (which is twice the apsidal angle as defined here) equals $2\pi/\sqrt{2} = 4.444\,28 = 2 \times 2.221\,44$, a value close to the one arrived at here. However, a comparison with the numerically derived result, also listed in Table 3, shows that the method proposed here is much more accurate: the two differ only in the fifth decimal place. As a comparison, we also show the apsidal angle for various values of small e using the p-ellipse approximation in the column labelled 'Numerical'.

From equation (26), we have

$$k = \sqrt{2}\left(1 - \frac{e}{2}\right)^{-1/2} \sim \sqrt{2}\left(1 + \frac{e}{4} + \cdots\right). \tag{50}$$

The apsidal angle is given by

$$\frac{\pi}{k} = \frac{\pi}{\sqrt{2}}\left(1 - \frac{e}{2}\right)^{1/2} \sim \frac{\pi}{\sqrt{2}}\left(1 - \frac{e}{4} - \frac{1}{32}e^2 + \cdots\right). \tag{51}$$

It is of interest to note that the roots can be found without any approximation for C in terms of the polylogarithmic function. For arbitrary C, one obtains from equation (45) an exact expression

$$-\frac{1}{C^2u^2}(\ln C^2 - E) - \frac{1}{C^2u^2}\ln\left(1 + \frac{1}{C^2u^2}\right) = \frac{h^2}{2C^2} \tag{52}$$

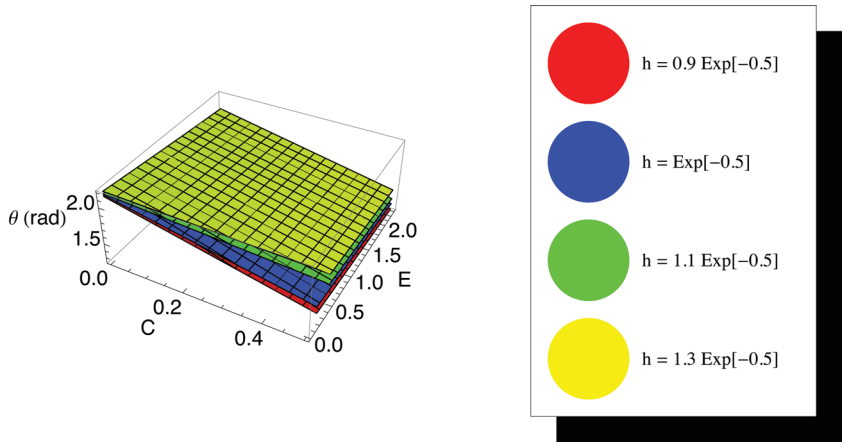

Figure 3. The apsidal angle in radians as a function of the core radius C and the energy E. Four different angular momenta are presented in different colours. See text for more details.

Table 3. The apsidal angle as calculated for different values of $u_c = 1/r_c$.

u_c	θ		
	Lambert W approximation	Numerical	Difference
1.0	2.063 10	2.063 00	0.000 10
1.1	2.071 22	2.071 16	0.000 06
1.2	2.078 68	2.078 62	0.000 06
1.3	2.085 58	2.085 54	0.000 04
1.4	2.092 01	2.092 00	0.000 01
1.5	2.098 03	2.097 97	0.000 06
1.6	2.103 68	2.103 61	0.000 07
1.7	2.109 01	2.108 96	0.000 05
1.8	2.114 05	2.113 97	0.000 08

for finding the roots of u^2. Now if we define $k \equiv \ln C^2 - E$ and $x \equiv -\frac{1}{C^2u^2}$, equation (52) reduces to

$$kx + x\ln(1-x) = \frac{h^2}{2C^2}\,, \tag{53}$$

$$k + \ln(1-x) = \frac{h^2}{2C^2}\frac{1}{x}\,, \tag{54}$$

$$k - Li_1(x) = \frac{h^2}{2C^2}\frac{1}{x}\,. \tag{55}$$

Here equation (55) is the functional equation of the polylogarithmic $Li_1(x) = -\ln(1-x)$ Lewin (1981) and

$$x = -\frac{1}{C^2u^2} = -\frac{r^2}{C^2}\,. \tag{56}$$

5 GRAVITATIONAL LENSING

The use of the Lambert W and the polylogarithmic functions to find the roots of equations such as equations (47) and (53) may have wider applicability. For example, we can use a similar approach to compute the deflection of a light ray by a logarithmic potential, useful in the context of gravitational lensing (Zwicky 1937; Cowling 1983; Schutz et al. 1990; Blundell et al. 2010) suggested that extragalactic nebulae offer a much better chance than stars for the observation of gravitational lens effects. Zwicky's idea was that some of the massive and more concentrated nebulae may be expected to deflect light by as much as half of an arcminute. Nebulae, in contrast to stars, possess apparent dimensions which are resolvable to very great distances. Zwicky was following up on the work of Einstein (1936) on stars acting as a gravitational lens. According to Zwicky, observations on the deflection of light around nebulae may provide the most direct determination of nebular masses (Smith 1936). Zwicky (1937) estimated the probability of detecting nebular galaxies which act as gravitational lenses and pointed out the possibility of ring-shaped images, flux amplification and understanding the large-scale structure of the Universe. The lensing equation can be generalized to three dimensions and cosmological distances by correction of the redshift-related distance (Schneider, Ehlers & Falco 1992).

For arbitrary K one has the following expression to determine the roots in the case of light deflection for a logarithmic potential:

$$V(r) = K\ln\left(r^2 + C^2\right)\,, \tag{57}$$

where K is a dimensionless constant and $r = \frac{1}{u}$.

For light deflection in the logarithmic potential considered, the differential equation for the given logarithmic potential is of the form

$$\frac{\mathrm{d}^2u}{\mathrm{d}\theta^2} + u = K\left(\frac{C^2u}{1+C^2u^2} - \frac{1}{u}\right) = \frac{-K}{u(1+C^2u^2)}\,. \tag{58}$$

The differential equation for small values of $C \ll 1$ reduces to

$$\therefore \frac{\mathrm{d}^2u}{\mathrm{d}\theta^2} + u - KC^2u = \frac{-K}{u}\,. \tag{59}$$

In the relativistic formulation (Hartle 2003), the differential equation for light deflection is

$$\left(\frac{\mathrm{d}\theta}{\mathrm{d}u}\right)^2 = \frac{1}{\frac{1}{b^2} - u^2 + 2Mu^3}\,, \tag{60}$$

$$\therefore u'' + u = 3Mu^2\,, \tag{61}$$

where b is the impact parameter.

Assuming the photon is a non-relativistic particle that travels at speed c and it is far from all sources of gravitational attraction (Hartle 2003), we can determine the light deflection $\Delta\theta$ produced by a logarithmic potential as

$$\Delta\theta = 2\int_0^{u_1} \frac{\mathrm{d}u}{\sqrt{1 - u^2 + K\ln\left(\frac{1}{u^2} + C^2\right)}}\,. \tag{62}$$

Table 4. The deflection angle $\Delta\theta$ (in arcseconds) as a function of k and C.

K	C	$\Delta\theta$
	1.0	0.004 44
10^{-8}	0.5	0.007 03
	0.0005	0.004 91
	1.0	2256.33
0.005	0.5	2861.51
	0.0005	3202.15
	1.0	69 637.4
0.25	0.5	95 986.9
	0.0005	109 909
	1.0	104 102
0.5	0.5	150 674
	0.0005	173 731
	1.0	142 042
1	0.5	218 327
	0.0005	251 802
	1.0	178 640
2	0.5	292 967
	0.0005	334 185

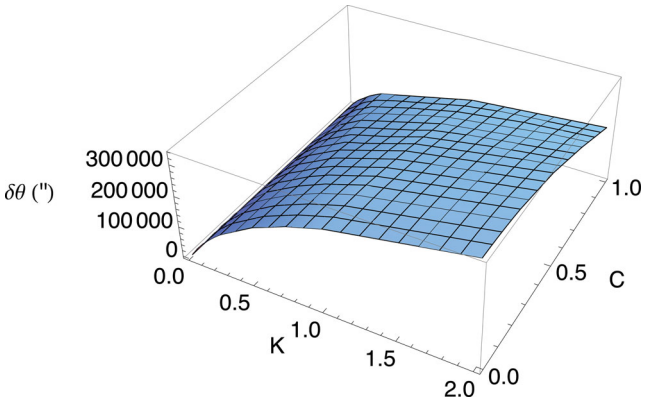

Figure 4. The deflection angle in arcseconds as a function of C and K. See text for more details.

Solving for the roots of the denominator, one obtains

$$1 - u^2 + K\left[\ln\left(1 + C^2u^2\right) - \ln u^2\right] = 0\,. \tag{63}$$

Solving for $K \ll 1$ by using the Lambert W function, we get

$$u^2 = \frac{1}{\left(\frac{1}{K} - C^2\right)} W_j\left\{\left(\frac{1}{K} - C^2\right) e^{\frac{1}{K}}\right\}, \tag{64}$$

where j denotes the branch of the Lambert W function.

The deflection angle is related to the Einstein angle $\theta_{\rm E}$ (Hartle 2003) which sets the characteristic angular scale for gravitational lensing phenomena. Gravitational lensing can be used to detect mass or energy in the Universe, whether visible or not. Table 4 shows the deflection angle for a range of values of K and C. Small K values produce small deflections, while smaller values of C produce larger ones, though with a weaker dependence. Fig. 4 shows the variation graphically.

Analogous calculations can be done for time-delay in light signals due to lensing galaxies Ohanian & Ruffini (1994). Intensity fluctuations caused by lumpy dark matter may provide direct observational existence for it. It is worth noting that the entire analysis can not only be done for the purely radial logarithmic potential, but also for equation (1) of the logarithmic potential, by considering the x and y components separately as was done for the gravitational potential (Bourassa & Kantowski 1975).

6 CONCLUSIONS

We have revisited and expanded the work of CS on orbits within a logarithmic potential. We did a comprehensive review of the Prendergast method used by CS. We performed an analytic and numerical study of the constants C_{-3}, C_{-2}, C_{-1}, C_0, C_1 and C_2 via a matrix which resulted in 18 equations for the six coefficients for the orbital Fourier-type series solution for values of U ranging from 0.1 to 1 which gave the unperturbed as well as perturbed solutions with better precision. The apsidal angle for the case of galactic orbits for a planar scale-free spherical logarithmic potential was obtained from the p-ellipse solution of the orbital differential equation and also the Lambert W function. Both the Lambert W and the polylogarithmic functions may have applications in problems involving exponential and/or logarithmic potentials such as gravitational lensing.

The Prendergast method, although not used as widely as others, has been quite useful in our analysis in Sections 2 and 3, and is likely to prove useful in the study of many types of galactic potentials.

Gravitational lensing can be used to detect mass in the Universe, whether dark or visible (Hartle 2003; Narlikar 2010). In general relativity, all energy curves space–time, and a constant vacuum energy produces a detectable curvature. Gravity may prove a useful tool for detecting and studying dark energy. The lensing due to the gravitational field of a black hole of background stars and galaxies (Thorne 1994) can be significant and the effects of a logarithmic potential warrant further study in this connection.

ACKNOWLEDGMENTS

We gratefully acknowledge discussions with Dr Seimenis during our work. We thank Curt Struck (Iowa State University) for sending earlier work on p-ellipse orbits. We also thank the anonymous referee for a stimulating review of our manuscript. SRV gratefully acknowledges research funding from King's University College at the Western University. This work was supported in part by the Natural Sciences and Engineering Research Council of Canada (NSERC).

REFERENCES

Belmonte C., Boccaletti D., Pucacco G., 2007, ApJ, 669, 202
Binney J., Spergel D., 1982, ApJ, 252, 308
Binney J., Tremaine S., 1987, Galactic Dynamics. Princeton Univ. Press, Princeton, NJ
Blundell K. M., Schechter P. L., Morgan N. D., Jarvis M. J., Rawlings S., Tonry J. L., 2010, ApJ, 723, 1319
Bourassa R. R., Kantowski R., 1975, ApJ, 195, 13
Chandrasekhar S., 1983, The Mathematical Theory of Black Holes. Clarendon Press, Oxford
Contopoulos G., Seimenis J., 1990, A&A, 227, 49 (CS)
Cowling S., 1983, PhD thesis, University College, Cardiff
Einstein A., 1936, Sci, 84, 506
Evans G. C., 1927, The Logarithmic Potential: Discontinuous Dirichlet and Neumann Problems. American Mathematical Society, Providence, Rhode Island
Evans N. W., 1993, MNRAS, 260, 191
Floquet G., 1883, Ann. Ec. Norm Suppl., 12, 47

Gerhard O. E., Binney J., 1985, MNRAS, 216, 467
Hagihara Y., 1931, Japan. J. Astron. Geophys., 8, 67
Hartle J. B., 2003, Gravity: An Introduction to Einstein's General Relativity. Addison-Wesley, San Francisco
Kamke E., 1943, Differential Gleichungen Losungsmethoden ung Losungen. Gesst & Portig, Leibzig
Karanis G. I., Caranicolas N. D., 2001, A&A, 367, 443
Lees J. F., Schwarzschild M., 1992, ApJ, 384, 491
Lewin L., 1981, Polylogarithms and Associated Functions. North-Holland, Amsterdam
Magnenat P., 1982, A&A, 108, 89
Miralda Escude J., Schwarzschild M., 1989, ApJ, 339, 752
Murray C., Dermott S., 1999, Solar System Dynamics. Cambridge Univ. Press, Cambridge
Narlikar J. V., 2010, An Introduction to Relativity. Cambridge Univ. Press, Cambridge
Ohanian H. C., Ruffini R., 1994, Gravitation and Spacetime. Norton, New York
Pfenniger D., de Zeeuw T., 1989, in Merritt D., ed., Dynamics of Dense Stellar Systems. Cambridge Univ. Press, Cambridge, England and New York, p. 81
Prendergast K., 1982, in Chudnovsky G. V., Chudnovsky D. V., eds, The Riemann Problem, Complete Integrability and Arithmetic Applications. Springer-Verlag, New York, p. 1
Pucacco G., Boccaletti D., Belmonte C., 2008, A&A, 489, 1055
Quigg C., Rosner J. L., 1977, Phys. Lett. B, 71, 153
Richstone D. O., 1980, ApJ, 238, 103
Richstone D. O., 1982, ApJ, 252, 496
Sachdev P. L., 1991, Nonlinear Ordinary Differential Equations and Their Applications. Cambridge Univ. Press, Cambridge
Schneider P., Ehlers J., Falco E. E., 1992, Gravitational Lenses. Springer-Verlag, Berlin
Schutz B. F., 1990, A First Course in General Relativity. Cambridge Univ. Press, Cambridge
Smith S., 1936, ApJ, 83, 23
Struck C., 2006, AJ, 131, 1347
Thorne K. S., 1994, Black Holes and Time Warps: Einstein's Outrageous Legacy. Norton, New York
Touma J., Tremaine S., 1997, MNRAS, 292, 905
Valluri S. R., Jeffrey D. J., Corless R. M., 2000, Can. J. Phys., 78, 823
Valluri S. R., Yu P., Smith G. E., Wiegert P. A., 2005, MNRAS, 358, 1273
Zwicky F., 1937, Phys. Rev. Lett., 51, 290

APPENDIX A: PERTURBED EQUATIONS

The following are the expressions for the components of equation (16):

$$S_{11} = E_6 - U^2 E_1 (\nu - 3)^2 \omega^2;$$
$$S_{13} = 0.5E_7 - 0.5U^2 E_2 \omega^2 (\nu - 1)^2 - 0.5U^2 E_4 \omega (\nu - 1);$$
$$S_{15} = 0.5E_8 - 0.5U^2 E_3 \omega^2 (\nu + 1)^2 - 0.5U^2 E_5 \omega (\nu + 1);$$
$$S_{22} = E_6 - U^2 E_1 (\nu - 2)^2 \omega^2;$$
$$S_{24} = 0.5E_7 - 0.5U^2 E_2 \omega^2 \nu^2 - 0.5U^2 E_4 \omega \nu;$$
$$S_{26} = 0.5E_8 - 0.5U^2 E_3 \omega^2 (\nu + 2)^2 - 0.5U^2 E_5 \omega (\nu + 2);$$
$$S_{31} = 0.5E_7 - 0.5U^2 E_2 \omega^2 (\nu - 3)^2 + 0.5U^2 E_4 \omega (\nu - 3);$$
$$S_{33} = E_6 - U^2 E_1 (\nu - 1)^2 \omega^2;$$
$$S_{35} = 0.5E_7 - 0.5U^2 E_2 \omega^2 (\nu + 1)^2 - 0.5U^2 E_4 \omega (\nu + 1);$$
$$S_{42} = 0.5E_7 - 0.5U^2 E_2 \omega^2 (\nu - 2)^2 + 0.5U^2 E_4 \omega (\nu - 2);$$
$$S_{44} = E_6 - U^2 E_1 \omega^2 \nu^2;$$
$$S_{46} = 0.5E_7 - 0.5U^2 E_2 \omega^2 (\nu + 2)^2 - 0.5U^2 E_4 \omega (\nu + 2);$$
$$S_{51} = 0.5E_8 - 0.5U^2 E_3 \omega^2 (\nu - 3)^2 + 0.5U^2 E_5 \omega (\nu - 3);$$
$$S_{53} = 0.5E_7 - 0.5U^2 E_2 \omega^2 (\nu - 1)^2 + 0.5U^2 E_4 \omega (\nu - 1);$$
$$S_{55} = E_6 - U^2 E_1 (\nu + 1)^2 \omega^2;$$
$$S_{62} = 0.5E_8 - 0.5U^2 E_3 \omega^2 (\nu - 2)^2 + 0.5U^2 E_5 \omega (\nu - 2);$$
$$S_{64} = 0.5E_7 - 0.5U^2 E_2 \omega^2 \nu^2 + 0.5U^2 E_4 \omega \nu;$$
$$S_{66} = E_6 - U^2 E_1 (\nu + 2)^2 \omega^2.$$

In the above expression for S_{22}, the bracketed term $(\nu - 2)$ has been corrected from the original form with $(\nu - 1)$ in CS.

The corresponding values of E are

$$E_1 = C^2 \left(0.375B^4 + 3B^2 + 1\right) + 0.5A^2 \left(0.5B^2 + B + 1\right);$$
$$E_2 = C^2 \left(3B^3 + 4B\right) + A^2 \left(0.375B^2 + B + 0.5\right);$$
$$E_3 = C^2 \left(0.5B^4 + 3B^2\right) + 0.5A^2 \left(0.5B^2 + B\right);$$
$$E_4 = 2\omega B \left(A^2 + 2C^2 + C^2B^2\right) + \omega B^2 \left(0.5A^2 + 2C^2B\right) - \omega B^3 C^2;$$
$$E_5 = \omega B^2 \left(A^2 + 2C^2 + C^2B^2\right) + \omega B \left(A^2 + 4C^2B\right);$$
$$E_6 = U^2\omega^2 B \left(A^2 + 3A^2B + 10C^2B + 2.5C^2B^3\right) + 0.75B^4 + 6B^2 + 2;$$
$$E_7 = U^2\omega^2 B \left(2A^2 + 2.5A^2B + 4C^2 + 13C^2B^2\right) + 6B^3 + 8B;$$
$$E_8 = U^2\omega^2 B \left(A^2 - A^2B + 2C^2B + 2C^2B^3\right) + B^4 + 6B^2.$$

In the above expression for E_4, the term with $0.5A^2$ has been corrected from its original form of $0.5A$ in CS.

This paper has been typeset from a TEX/LATEX file prepared by the author.